Desalination and Water Treatment
www.deswater.com

doi: 10.1080/19443994.2015.1036363

57 (2016) 10312–10323
May

Taylor & Francis
Taylor & Francis Group

Fabrication and application of an immobilized TiO_2/chitosan layer-by-layer system loaded with Reactive Red 4 dye for the removal of phenol and its intermediates

S. Sabar[a,*], M.A. Nawi[b]

[a]*Chemistry Section, School of Distance Education, Universiti Sains Malaysia, 11800 Minden, Penang, Malaysia, Tel. +60 4 6535924; email: sumiyyahs@usm.my*
[b]*School of Chemical Sciences, Universiti Sains Malaysia, 11800 Minden, Penang, Malaysia, Tel. +60 4 6534031; email: masri@usm.my*

Received 18 February 2014; Accepted 23 March 2015

ABSTRACT

An immobilized TiO_2/chitosan loaded with Reactive Red 4 (RR4) dye has been successfully fabricated via a layer-by-layer assemblage system. The immobilized photocatalyst was prepared by adsorbing RR4 dye on a chitosan (CS) sub-layer supported by a glass plate, before being coated with TiO_2 as the top layer (known as TiO_2/RR4-CS/glass). This layer-by-layer assemblage system allows the dye to be in contact with the TiO_2/CS interface. In addition, the leaching as well as direct oxidation of the chemisorbed dye would also be prevented. Photo-etching of the immobilized TiO_2/RR4-CS system for at least 10 h increased its surface area and enhanced its photocatalytic activity due to the formation of macropores within the TiO_2 top layer. Application of the immobilized TiO_2/RR4-CS layer-by-layer system shows that the photocatalytic system exhibited high photocatalytic efficiencies under the irradiation of a 45 W compact fluorescent lamp for the degradation of phenol as well as its intermediates. In addition, the immobilized photocatalyst system was also reusable for at least five cycles of extended use without losing its efficiency. The immobilized TiO_2/RR4-CS layer-by-layer system improved the photocatalytic activity of TiO_2 due to its better charge separation and lower electron–hole pair recombination.

Keywords: Photocatalysis; Titanium dioxide; Immobilization; Dye loaded; Reactive Red 4; Charge transfer

1. Introduction

Titanium dioxide (TiO_2) is the most efficient photocatalyst when compared to other semiconductors since it is chemically and biologically inert, photocatalytically and thermally stable, relatively easy to produce and to use, cheap and safe towards both humans as well as the environment. Its strong oxidizing agent is capable of degrading organic pollutants (such as dyes, polymers, pesticides, and herbicides) present at or near the surface of the TiO_2 resulting usually in their complete mineralization into H_2O and CO_2 by irradiation with UV light. However, its large band gap energy (~3.2 eV) usually results in low degradation rates and quantum efficiency of the system under solar and visible light region.

---

*Corresponding author.

Modification of TiO_2 such as doping with metal ions [1,2], doping with non-metal elements [2–4], and dye modifying [5–9] can improve the photocatalytic performance of TiO_2. The modification of TiO_2 with dye has been reported to be the most effective way to extend the photoresponse of TiO_2 into the visible region. Several studies have reported that photosensitization is the main mechanism in the dye-modified TiO_2 photocatalyst system [5–8]. In this case, the dye would get excited, by absorbing photon energy, and produce electrons which were then transferred to the conduction band of TiO_2. However, according to Hilal et al. [9], dye-sensitized TiO_2 has two characteristic features: they are sensitized to longer wavelengths (e.g. visible) and they oxidize contaminants demanding oxidation potentials less than the dye valence band edge only. If the dye fails to sensitize TiO_2 under visible light irradiation, the mechanism may be a charge transfer process rather than photosensitization [9].

Generally, the dye is either physically mixed with the photocatalyst [5,6] or directly adsorbed on the surface of the photocatalyst [7–9]. However, the interaction between the dye and the photocatalyst in such techniques is not stable and may cause leaching or desorption of the dye. Besides this, direct exposure of the dye to light irradiation leads to fast decomposition or photobleaching of the dye during the photoreaction and thus, affects the photocatalytic degradation of the organic pollutants [6,8,10]. In addition, the photobleaching of the dyes also produces intermediates which also needed to be treated and disposed of [6]. Furthermore, the use of dye-modified TiO_2 in suspension mode causes problems in the regeneration, recovery, and reuse of the dye and the photocatalyst. Attempts to immobilize the dye on solid supports fail to maintain the sustainability of the dye-modified TiO_2 system upon regeneration [10].

The main objective of this study is to fabricate an immobilized TiO_2/chitosan loaded with Reactive Red 4 (RR4) dye via a layer-by-layer assemblage system. The layer-by-layer assemblage system consists of TiO_2 as the top layer, the chemisorbed dye on chitosan (CS) as the sub-layer, and glass plate as the supporting material (known as TiO_2/RR4-CS/glass). CS was selected as the immobilization substrate for the dye since the amino-function of the CS allows binding, including adsorption or immobilization of dyes [11–13]. On the other hand, RR4 is a conventional and inexpensive dye used in the textile industry. It is a highly stable tetrasulfonated monoazo dye that can strongly bind with amine groups of CS via electrostatic attraction [12]. Its chemical structure is given in Fig. 1. The immobilized TiO_2/RR4-CS layer-by-layer system will be applied for the photocatalytic degradation of phenol as well as its intermediates under irradiation of a 45 W compact fluorescent lamp. The layer-by-layer assemblage system would be expected to offer many advantages such as enhancing the photocatalytic activity of TiO_2, sustainable, low in energy, and expenses, as well as clean to the environment.

2. Materials and methods

2.1. Materials

TiO_2 (99% anatase), chitosan (CS) flake (68.2% degree of deacetylation with a molecular weight of 322 g mol^{-1}), and Reactive Red 4 (RR4) with 50% dye content (Color Index Number: 18105, chemical formula: $C_{32}H_{23}ClN_8Na_4O_{14}S_4$, MW: 995.23 g mol^{-1}, λ_{max}: 517 nm) were purchased from Sigma-Aldrich. Maleic acid (≥99%) and fumaric acid (≥99%) were supplied by Merck. Other chemicals used were phenol (Scharlau, 99.5%), phenol formaldehyde powder resin (PF) (Borden Chemical (M) Sdn. Bhd.), epoxidized natural rubber (ENR_{50}) (Kumpulan Guthrie Berhad), hydroquinone (Acros, 99%), and catechol (Fluka, >98%). All chemicals were used without additional purification. Ultra-pure water (18.2 MΩ cm^{-1}) was used in this work.

2.2. Preparation of immobilized CS

CS solution was prepared by dissolving 6.0 g of CS flakes in 400 ml of 5% acetic acid aqueous solution in a ball mill grinder for 30 h at 60 rpm. The produced white viscous CS solution was cast evenly on the surface of the glass plates, each with a dimension of 4.7 cm × 6.5 cm (length × height), and dried completely at room temperature (27˚C). A CS loading of 0.65 ± 0.08 mg cm^{-2} was used throughout this study as this is the optimum loading of CS obtained for the adsorption of RR4 dye [12]. The fabricated immobilized CS on glass plates appeared white in color and is hereafter known as CS/glass.

2.3. Preparation of RR4-CS plates

Immobilized RR4-CS plates were prepared by conditioning the CS/glass plates in ultra-pure water at pH 4.0 for 1 h, followed by the adsorption process in 100 mg L^{-1} RR4 dye solution at pH 6.0. A detailed study on the adsorption of RR4 dye by the immobilized CS/glass has been reported by Nawi et al. [12]. The dye solution was repeatedly changed with a new batch until CS has become fully saturated. These

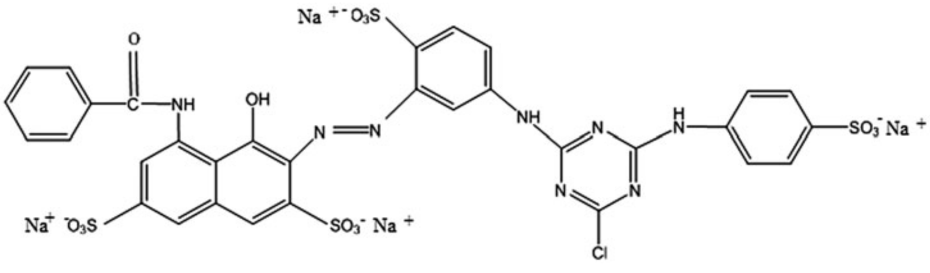

Fig. 1. Chemical structure of Reactive Red 4 (RR4) dye.

plates henceforth are referred to as RR4-CS/glass. The fully saturated adsorption amount of RR4 by CS was 172 mg g^{-1} (1.10×10^{-3} mol m^{-2}) and used throughout this study unless otherwise stated.

2.4. Preparation of immobilized TiO_2 layer

The photocatalyst formulation was prepared according to the previously reported method by Jawad and Nawi [14]. In this case, a fixed amount of 5.0-g ENR_{50} solution (~11.3% w/v of ENR_{50} in toluene) was added into an amber bottle which contained 12.0 g of TiO_2 powder. Next, 0.15 g of PF was added to the mixture. Finally, 60 mL of acetone was poured into the bottle before being sonicated for 5 h in order to produce a homogenized emulsion without any agglomeration. This TiO_2 formulation was used to immobilize TiO_2 on a glass substrate, CS/glass, and/or RR4-CS/glass by a simple dip-coating method. Different loadings of TiO_2 were obtained by varying the number of dip-coating processes, where a single dip of coating has the equivalent weight of 0.33 ± 0.08 mg cm^{-2}. The coated substrates hereafter are called as TiO_2/glass, TiO_2/CS/glass, or TiO_2/RR4-CS/glass systems, respectively.

2.5. Instruments

A HACH DR/2000 Direct Reading Spectrophotometer was used to monitor the concentrations of RR4 dye during the adsorption process at a wavelength of 517 nm. The concentration of phenol and its intermediates was followed by a high performance liquid chromatography (HPLC) on the JASCO HPLC system, consisting of PU-1580 Intelligent HPLC pump equipped with a UV-1570 intelligent UV/Vis detector. Chromatographic separation was accomplished on a Supelcosil C18 reverse phase column (Supelcosil, 25 cm × 4.6 mm, 5 μm) at 25˚C and monitored at 220–380 nm. The mobile phase used was a mixture of methanol (chromatography grade) and ultra-pure water at a ratio of 60:40 v/v pumped at a flow rate of 0.5 mL min^{-1}. Total organic carbon (TOC) analysis to analyze the residual carbon content was determined in a Shimadzu TOC-V CPH/CPN Analyzer. TOC analysis was conducted on the photocatalyst systems (TiO_2/glass, TiO_2/CS/glass, and TiO_2/RR4-CS/glass) in order to determine the leaching of organic carbon from the prepared plates. A radiometer (model PMA 2100 from Solar light Co. Inc.) equipped with PMA 2110 UV-A (320–400 nm) and PMA 2106 UV-B (280–320 nm) detectors was used to determine the UV irradiance leakage from the 45 W compact fluorescent lamp. The irradiance spectrum of the light source was measured with an ASD FieldSpec HandHeld 2 portable Spectroradiometer (Analytical Spectral Devices Inc.) covering wavelengths from 325 to 1,075 nm.

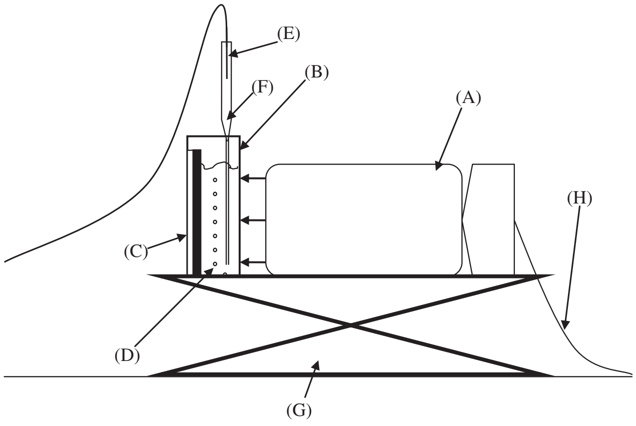

Fig. 2. Schematic diagram of experimental setup for the photocatalytic system: (A) 45 W compact fluorescent lamp, (B) glass reactor cell, (C) immobilized plate, (D) phenol aqueous solution, (E) aeration supplied by an aquarium pump attached by a PVC tube, (F) Pasteur pipette, (G) scissor Jack, and (H) power supply.

2.6. Irradiation system setup

The schematic diagram of the experimental setup for the photocatalytic system is shown in Fig. 2. The immobilized plates were placed upright in a custom-made glass reactor cell with dimensions of 5 cm × 8 cm × 1 cm (length × height × width) that can hold up to 20 mL of phenol solution. An aerator made from an aquarium pump was attached to the container via a PVC tube for a supply of air and proper agitation of the solution for solutes transport purposes. The system was irradiated with a 45 W compact fluorescent lamp with an emitted UV intensity of 4.0 W m^{-2} and main peak emission wavelengths centered at 402 (weak), 434 (weak), 486 (weak), 545 (strong), and 611 nm (moderate). This lamp was placed horizontally to be in contact with the outer surface of the glass reactor cell.

2.7. Kinetic analysis

HPLC was used to measure the concentrations of phenol and its intermediates in the aliquots that were syringed out (0.5 mL sample) from reaction mixtures and measured at 20 min time intervals for 2 h. The percentage of phenol remaining (%) is defined as:

$$\text{Phenol remained} = \left(\frac{C_t}{C_o}\right)100 \tag{1}$$

where C_t and C_o are the concentrations at the irradiation time t (min) and the initial concentration of phenol (mg L^{-1}), respectively. The Langmuir–Hinshelwood kinetic model was used to determine the pseudo-first-order rate constant or degradation rate, and the equation is given by [15]:

$$\ln\left(\frac{C_o}{C_t}\right) = -kt \tag{2}$$

where C_o and C_t are the initial concentrations of phenol and the concentrations at irradiation time t (min) in mg L^{-1}, respectively. The pseudo-first-order rate constant, k (min^{-1}), was calculated from the slope of plots ln (C_o/C_t) vs. t.

The photocatalytic degradation of phenol was performed using 20-mL volumes of 10-mg L^{-1} phenol solutions under room temperature at an ambient pH (6.6) and an aeration flow rate of 40 mL min^{-1}. The immobilized plates after each cycle (each cycle = 2 h) were recovered, washed with ultra-pure water for 30 min (to remove accumulated pollutants on the surface of the photocatalyst), and reused up to five cycles to study the reusability of the immobilized photocatalyst systems. All experiments were conducted in triplicates under identical conditions, and the results are reported as average.

3. Results and discussion

3.1. Optimization of TiO_2 loading

In this work, immobilized TiO_2/chitosan loaded with RR4 dye has been fabricated in order to enhance the photocatalytic activity of TiO_2. In contrast to most of the published literature [5–9], the dye was not mixed with TiO_2, but rather anchored on the CS sublayer underneath the TiO_2 top layer in a layer-by-layer assemblage system. In this way, the dye would be protected from direct irradiation and thus could remain longer within the photocatalyst system.

Optimization of the TiO_2 loading is significant in order to avoid the use of excessive catalyst and to ensure total absorption of efficient photons. A series of TiO_2 loadings ranging from 0.33 to 3.27 mg cm^{-2} were obtained by varying the number of dip-coatings on top of the RR4-CS layer. In the dip-coating processes, the TiO_2 loading and thickness increases almost linearly with an increase in the number of times the support substrate is dipped into the coatings formulation [16]. In this study, a single dip has the equivalent weight of 0.33 ± 0.08 mg cm^{-2} of immobilized TiO_2 with a thickness of 8.71 ± 0.32 μm [17].

Fig. 3 shows the pseudo-first-order rate constants or degradation rates of phenol by the TiO_2/RR4-CS layer-by-layer system at different loadings of TiO_2. From the graph, it can be observed that the

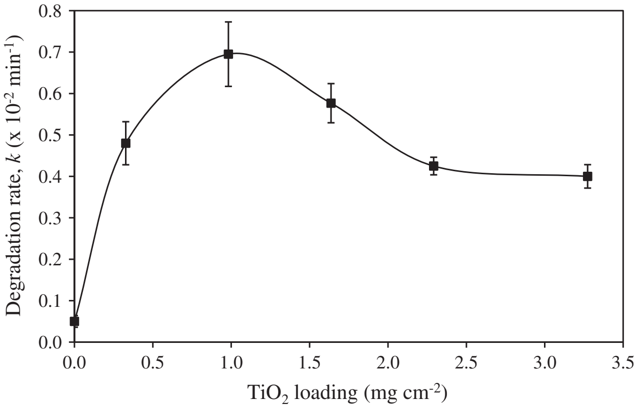

Fig. 3. The effects of TiO_2 loading on the photocatalytic degradation of phenol by the TiO_2/RR4-CS/glass system at ambient pH (6.6) with initial phenol concentration of 10 mg L^{-1}.

photocatalytic performance of the TiO_2/RR4-CS layer-by-layer system can be remarkably improved with an increase in the TiO_2 loading up to the optimum loading of 0.98 mg cm^{-2} (equivalent to 14.5 ± 0.4 μm of thickness [17]). At such loading or thickness, about 75.0% of the phenol was degraded after 2 h of irradiation. It has been reported that there was an optimum film thickness under which the rate of reaction is at its maximum because the fraction of light absorbed reaches 100% [18].

However, it can be observed that the degradation rates slowed down beyond the optimum loading and then leveled off. This is because high loading of a TiO_2 photocatalyst would result in a thicker, denser, and less porous TiO_2 layer which would hinder the mobility and diffusion of phenol molecules towards the TiO_2/RR4-CS interface [17]. Furthermore, the light scattering effect also increased, which made the inner layer of the TiO_2 unavailable to harvest maximum incident light. This reduced the light penetration towards the dye since it has to first move some distance within the TiO_2 layer itself before it can reach the interface of TiO_2/RR4-CS [19]. If the photons and oxidative radicals cannot reach the interface of TiO_2/RR4-CS, the RR4 dye will not be oxidized. In fact, it was also reported that the recombination of unreacted electrons and hole pairs produced by irradiation could be enhanced by the large amount of photocatalyst present [20].

Below the optimum loading, there is weak absorption of light and less production of oxidative radicals due to the thin TiO_2 layer. Besides that, the degradation rate of phenol at 0.98 mg cm^{-2} of TiO_2 loading was 14 times faster than without the presence of the catalyst. Without the photocatalyst, there were no oxidative radicals available to degrade the phenol and oxidize the chemisorbed RR4 dye within the immobilized RR4-CS layer. This fact eliminated the possible degradation of phenol by the dye itself as it needed the TiO_2 to initiate the electron transfer processes. Therefore, 0.98 mg cm^{-2} was selected as the best TiO_2 loading since the thickness at this loading allowed the generated oxidative radicals to be as close as possible to the TiO_2/RR4-CS interface. Hence, the oxidative radicals can easily oxidize the chemisorbed RR4 dye, followed by a fast electron transfer to the TiO_2 layer, leading to an efficient charge separation. At this point, charge separation is more dominant than charge recombination.

A similar observation was also reported by Shang et al. [19] in the photocatalytic performances of glass/SnO_2/TiO_2 interface composite film for the degradation of formaldehyde. On the other hand, Nawi and Sabar [17] has obtained an optimal TiO_2 loading of 0.33 mg cm^{-2} for the photocatalytic degradation of RR4 by the TiO_2/CS layer-by-layer system. According to the authors, the highest synergistic effect was observed at this optimum loading since it offered better adsorption of RR4 by CS sub-layer combined with reasonable light absorption to produce sufficient amounts of oxidative radicals on the surface of the TiO_2 for the simultaneous photocatalytic degradation of the nearby RR4 dye anions.

In contrast, an earlier study by Nawi et al. [21] reported that the oxidation of the CS sub-layer was observed when combined with TiO_2 in a layer-by-layer system under an extended irradiation period (≥10 h irradiation) in ultra-pure water [21]. However, the oxidation of the CS sub-layer would highly depend on the amount of coated TiO_2 photocatalyst. This is because the increase in the TiO_2 loading increases the amount of the generated oxidative radicals [22]. Fig. 4 shows the UV–vis DRS spectra of CS sub-layer oxidized at different TiO_2 loadings after they were irradiated in ultra-pure water for five cycles (equivalent to 10 h) without the presence of RR4 dye. As can be seen, un-irradiated and irradiated CS with a TiO_2 loading of 0.33 and 0.98 mg cm^{-2} has an absorption band at 300 nm, which is caused by the $n \rightarrow \sigma^*$ transition of amino groups in CS. Irradiated CS with a TiO_2 loading of 1.30 mg cm^{-2} or more exhibited two absorption bands. The first absorption band shows a 10-nm redshift compared to the original CS. The other absorption band at 368 nm is assigned to the $n \rightarrow \pi^*$ transition of carbonyl or carboxyl groups, which indicates that a new side group was formed during the oxidation process [21,23,24]. The intensity of this peak increases with the increase in TiO_2 loading which is

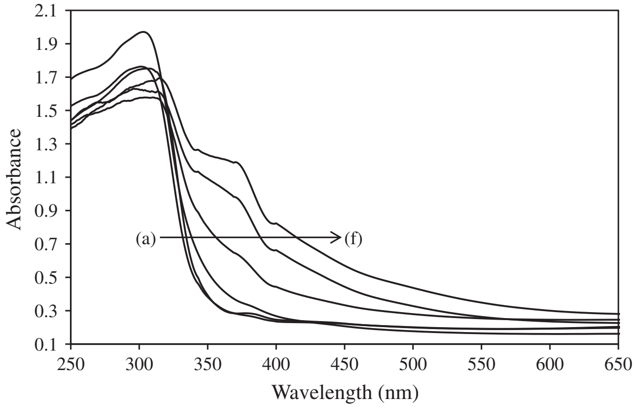

Fig. 4. UV–vis DRS spectra of (a) un-irradiated CS/glass and irradiated CS/glass at (b) 0.33, (c) 0.98, (d) 1.30, (e) 2.29, and (f) 3.27 mg cm^{-2} TiO_2 loading in the TiO_2/CS layer-by-layer system for five cycles (10 h) in ultra-pure water.

attributed to the increase in the concentration of carbonyl groups. This observation is consistent with the browning effect (caused by the formation of carbonyl chromophore [21,23–25]) on the irradiated CS, whereby the color becomes more intense at a higher loading of TiO_2. Thus, it can be concluded that increasing the TiO_2 loading increases the oxidation of the CS sub-layer.

From this point of view, increasing the TiO_2 loading would be expected to increase the oxidation of chemisorbed RR4 dye in the TiO_2/RR4-CS layer-by-layer system. However, as depicted by Fig. 3, increasing the TiO_2 loading beyond the optimum loading of 0.98 mg cm^{-2} decreases the degradation rates of phenol. This is because the oxidative radicals produced from the oxidation of chemisorbed RR4 could not be transported efficiently to the pollutant in the bulk solution due to the thickness of the TiO_2 layer. The thick TiO_2 layer increases the distance of electron transfer from the interface TiO_2/RR4-CS to the surface of TiO_2 top layer. It was also observed that the oxidation of the CS sub-layer only occurred when the loading of the TiO_2 layer immobilized on the CS sub-layer was more than 1.30 mg cm^{-2}. Therefore, the effect of the oxidized CS sub-layer on the photocatalytic degradation of phenol by the TiO_2/RR4-CS layer-by-layer system did not arise in this study since the optimum loading of TiO_2 in this work was only 0.98 mg cm^{-2}. The selected optimum loading is sufficient to cause the oxidation of chemisorbed RR4 and degrades phenol without oxidizing the CS sub-layer.

3.2. Leachability of dissolved organic matter via TOC analysis

Since the binders used for immobilizing the photocatalyst were organic polymers in the form of ENR_{50} and PF, the possibility of leached dissolved organic matter (DOM) should be investigated. The leached DOM from the fabricated TiO_2, TiO_2/CS, and TiO_2/RR4-CS layers during the photocatalytic reaction were evaluated by the TOC analysis. In this regard, the immobilized photocatalyst systems (TiO_2/glass, TiO_2/CS/glass, and TiO_2/RR4-CS/glass) were immersed in ultra-pure water and irradiated with a 45 W compact fluorescent lamp. After 2 h of irradiation (equivalent to one cycle), the water samples were collected and replaced with a new batch of ultra-pure water using the same respective immobilized photocatalyst plates. This procedure was repeated until the seventh cycle.

The results of the TOC analysis as a function of repeated cycles of irradiation are presented in Fig. 5. The concentrations of TOC in the water samples for all of the immobilized photocatalyst systems demonstrated the same trend. The concentrations were initially high in the first cycle, but gradually decreased and gave almost zero values after the fifth cycle of irradiation. High TOC indicates the presence of high organic matters in the water samples. From the observation, there are three possible sources of organic matters from the TiO_2/RR4-CS layer-by-layer system: (1) degradation of organic binders (ENR_{50}) applied as adhesive in the TiO_2 formulation, (2) leaching of CS sub-layer, and (3) photobleaching of chemisorbed RR4 dye.

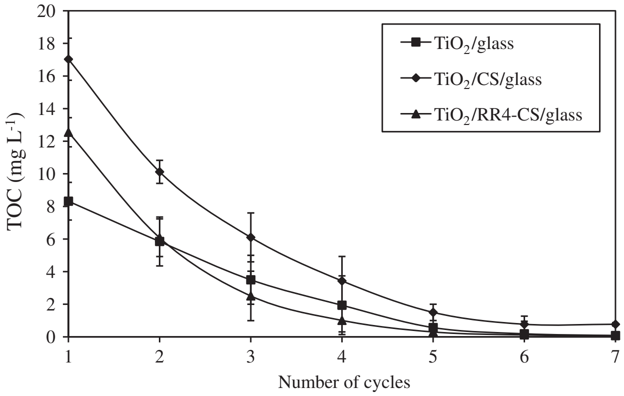

Fig. 5. TOC (mg L^{-1}) values of irradiated water samples representing the leachability of organic matters from the TiO_2, TiO_2/CS, and TiO_2/RR4-CS layers during repeated cycles of irradiation.

ENR_{50} used as an adhesive in the TiO_2 formulation is not photoresistant and degrades during the photocatalytic reaction. This is supported by the fact that the TiO_2 single layer system contributes about 8.32 ± 1.15 mg L^{-1} of TOC at the first cycle of irradiation. Similar observations were also made by others [14,26,27]. However, the degradation of the ENR_{50} binder by the photocatalytic reaction is an advantage since it can enhance the porosity and surface area of the immobilized photocatalyst [27,28].

Like other polysaccharides, CS is sensitive to various types of irradiation [21,23,24,29–32]. The CS sub-layer is leachable upon irradiation with light and increases the concentration of DOM in the treated water samples. From Fig. 5, it is believed that the leaching of the CS sub-layer combined with the degradation of the ENR_{50} binder is responsible for the increase in TOC by the TiO_2/CS layer-by-layer system. The concentration of TOC for the TiO_2/CS layer-by-layer system at the first cycle was 17.03 ± 1.29 mg L^{-1}. Overall, the TiO_2/CS layer-by-layer system maintains higher TOC as compared to TiO_2 single layer and TiO_2/RR4-CS layer-by-layer systems from the first to the seventh cycle. In fact, the TiO_2/CS layer-by-layer system continued to leach out organic matters into the treated water samples as shown by the detected TOC values.

On the other hand, one of the drawbacks of a dye-modified photocatalytic system is the photobleaching of the dye that could also contaminate the treated water samples. The mineralization of the dye is a complex quantity, which is governed by the desorption of dye from the catalyst surface and degradation of the dye [6]. Generally, the degradation of RR4 arises from the cleavage of azo bonds and the opening of the aromatic rings due to the hydroxylation by the attack of hydroxyl radicals. The resulting intermediate metabolites (e.g. aromatic amine or phenolic compounds) were further degraded to organic acids, inorganic ions (NO_3^-, Cl^- and SO_4^{2-}) as well as H_2O and CO_2. Subsequent irradiation of the TiO_2/RR4-CS layer-by-layer system causes a gradual disappearance in the intensities of the visible bands of RR4 under prolonged irradiation due to the breaking of the azo bonds [17]. However, from the HPLC and ion chromatographic analyses, there was no trace of RR4 intermediates and inorganic ions detected. This could either mean that a very low amount of RR4 was photobleached during the irradiation of the TiO_2/RR4-CS layer-by-layer system or that the intermediates produced from the degradation of RR4 dye could be readsorbed on the surface of the CS sub-layer. This hypothesis is consistent with the TOC analysis of the TiO_2/RR4-CS layer-by-layer system. The TOC value of the TiO_2/RR4-CS layer-by-layer system (12.55 ± 0.89 mg L^{-1}) was in fact lower than that obtained by the TiO_2/CS layer-by-layer system. This is because less CS is accessible for degradation as it is electrostatically attached to the RR4 dye. Hence, the TOC value contributed by the TiO_2/RR4-CS layer-by-layer system was mainly from the degradation of ENR_{50} binder, with minor influence from the CS and RR4 dye.

After the fifth cycle, negligible TOC was obtained for all the respective photocatalyst systems indicating that most of the major organic compounds have been degraded, leaving only those hidden behind and in contact with the TiO_2 top layer. Besides that, the intermediates produced from the degraded organic compounds were mineralized to harmless acid, H_2O, and CO_2 after the fifth cycles. Therefore, in order to apply the immobilized photocatalyst systems without the interference from the degradation of DOM by the fabricated plates, the plates need to be subjected to a "photo-etching" for about 10 h of irradiation under a 45 W compact fluorescent lamp in ultra-pure water [26].

3.3. Effect of photo-etching

The immobilization process is known to reduce intrinsically the active surface area available for adsorption and catalysis through the formation of non-porous layers [33]. Photo-etching of the immobilized photocatalyst system by irradiation under light would lead to the formation of macropores within the TiO_2 layer as recently been observed by Nawi et al. [28]. They reported that macropores were generated within the TiO_2 top layer in the TiO_2/CS layer-by-layer system after the third cycle of irradiation by light and are completely formed after the fifth cycle (one cycle is equivalent to 2 h of irradiation). The macropores were generated due to the degradation of the ENR_{50} binder which acted as a macro-pore forming agent on the surface of TiO_2 layer [28]. The generation of macropores would highly improve the photocatalytic performance of the immobilized TiO_2 photocatalyst system. In order to study the effect of photo-etching on the immobilized photocatalyst for the photocatalytic degradation of phenol, the TiO_2/RR4-CS layer-by-layer system was irradiated under a 45 W compact fluorescent lamp in ultra-pure water for a total of 10 h or five cycles.

As shown in Fig. 6, the irradiated TiO_2/RR4-CS/glass could effectively remove phenol better than the un-irradiated TiO_2/RR4-CS/glass where the percentage of phenol that remained after 2 h of irradiation was 1.70 ± 0.03% and 27.1 ± 1.3%, respectively. In addition, the degradation rate of phenol by the irradiated TiO_2/RR4-CS/glass (0.0304 ± 0.0002 min^{-1}) was more than four times faster than un-irradiated TiO_2/RR4-CS/glass (0.0072 ± 0.0006 min^{-1}).

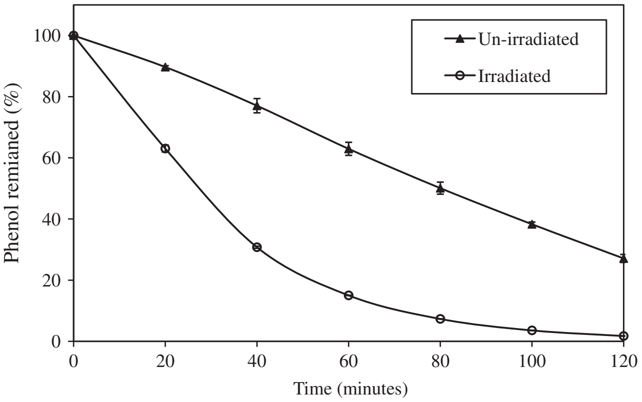

Fig. 6. The effect of un-irradiated and irradiated TiO_2/RR4-CS layer-by-layer systems on the photocatalytic degradation of phenol at ambient pH (6.6) with TiO_2 loading of 0.98 mg cm^{-2} and initial phenol concentration of 10 mg L^{-1}.

The inefficiency of un-irradiated or un-etched TiO_2/RR4-CS/glass in degrading phenol was due to the masking effect of the TiO_2 outer layer that blocks the RR4-CS sub-layer. Without the generation of macropores, the layer-by-layer system effectively behaved like the TiO_2 single layer. This is because the RR4-CS sub-layer was isolated from phenol molecules by the TiO_2 top layer, hindering the penetration of hydroxyl radicals and the diffusion of pollutants. Thus, the dye in the sub-layer provided a less contribution to the reaction as it was unable to participate in the electron or an energy transfer process. Generation of macropores increased the light penetration and allowed better diffusion of the pollutants as well as hydroxyl radicals across the inner layer of the TiO_2 [14,28], hence increasing the photonic efficiency at the TiO_2/RR4-CS interface.

In fact, Nawi et al. [26] as well as Nawi and Zain [27] have also reported that the degradation of the ENR_{50} binder in the TiO_2–ENR_{50}–PVC coating formulation increases the surface area of the immobilized TiO_2 anatase and Degussa P-25, respectively. In addition, high leaching of DOM from the ENR_{50} binder, CS sub-layer, and chemisorbed RR4 dye would decrease and mostly stopped upon the fifth cycle of irradiation as discussed earlier (Section 3.2). Therefore, all the immobilized photocatalyst plates were photoetched for at least 10 h of irradiation under a 45 W compact fluorescent lamp in ultra-pure water prior to its application in the photocatalytic degradation of phenol. This is to generate macropores on the TiO_2 top layer and to avoid leaching of DOM as well as any other possible interferences from the photocatalyst samples on the target phenol pollutant.

3.4. Control experiments

Control experiments were conducted to evaluate the effect of loading RR4 dye at the TiO_2/CS interface by comparing the photolysis, adsorption, and photocatalytic performance of the system against the other immobilized systems. Experiments conducted in the dark (adsorption) using different immobilized systems (TiO_2/glass, TiO_2/CS/glass and TiO_2/RR4-CS/glass) showed no significant phenol loss. As shown in Fig. 7, control experiment conducted under light irradiation in the absence of the immobilized system (photolysis) was extremely poor with only 6.0 ± 2.8% of phenol removal. In the presence of the photocatalyst under light irradiation, 82.1 ± 1.2% and 86.1 ± 8.8% of phenol were degraded within 2 h of treatment by the TiO_2/glass and TiO_2/CS/glass, respectively. Meanwhile, almost 100% of phenol was removed by the TiO_2/RR4-CS/glass under the same conditions. This proved that the immobilized TiO_2/CS layer-by-layer system loaded with RR4 dye improved the photocatalytic degradation of phenol.

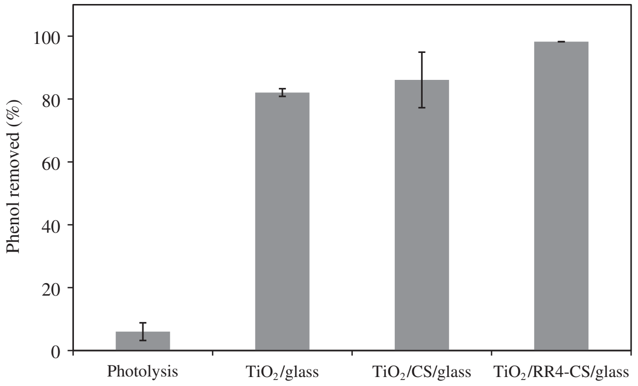

Fig. 7. Control experiments for the photocatalytic degradation of phenol by the TiO_2/glass, TiO_2/CS/glass, and TiO_2/RR4-CS/glass systems at ambient pH (6.6) with TiO_2 loading of 0.98 mg cm^{-2} and initial phenol concentration of 10 mg L^{-1}.

The mechanism of the immobilized TiO_2/RR4-CS layer-by-layer system can be explained by the effect of a charge transfer process rather than photosensitization [17]. In the presence of TiO_2 as the top layer, the electrons in the TiO_2 particles were excited to produce conduction band electrons (eCB^-) and valence band holes (hVB^+). This explains the removal of phenol by the TiO_2/glass system which is illustrated in Fig. 8(a). The photo-generated holes reacted with H_2O or OH^- ions to produce hydroxyl radicals ($OH^\cdot$), which are a very strong oxidant. The $OH^\cdot$ radicals, derived from the TiO_2 surface, diffused through the porous TiO_2 top layer and oxidized the chemisorbed RR4 dye. The oxidation of chemisorbed RR4 dye, by the $OH^\cdot$ radicals at the TiO_2/CS interface, generates electrons which were then transferred to the conduction band of TiO_2. This would result in the build-up of excess electrons in the conduction band of TiO_2. Consequently, the accumulation of excess electrons in the TiO_2 were scavenged by molecular oxygen to form superoxide radicals ($O_2^{\cdot-}$) and hydroperoxyl radicals ($^\cdot OOH$). These radicals attacked the phenol aromatic ring forming intermediates and eventually mineralizing them to CO_2 and H_2O. The electron transfer process improved the charge separation and decreased the recombination rate of photoinduced electron–hole pairs on the surface of TiO_2. Fig. 8(b) illustrates the overall mechanisms involved during the photocatalytic degradation of phenol by the immobilized TiO_2/RR4-CS layer-by-layer system.

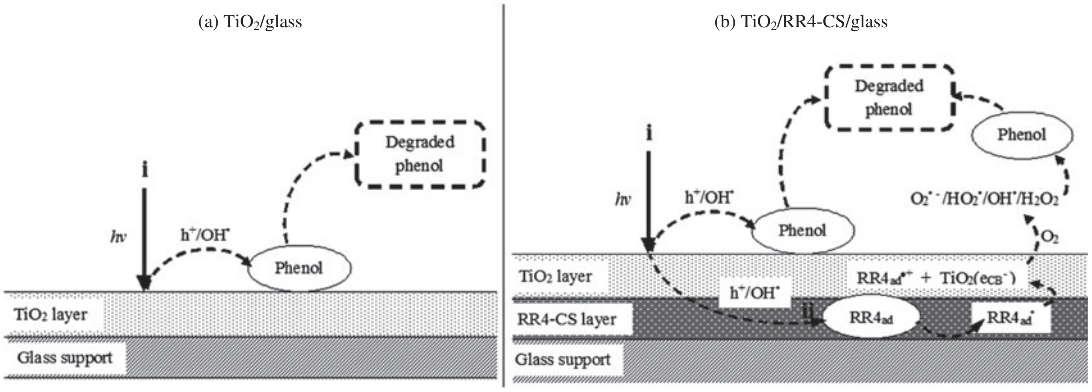

(i) Direct photocatalytic degradation of phenol by the TiO_2 photocatalyst.
(ii) Charge transfer from the oxidation of chemisorbed RR4 dye at the TiO_2/RR4-CS interface to the conduction band of TiO_2.

Fig. 8. Illustration of the possible mechanisms involved during the photocatalytic degradation of phenol by the (a) TiO_2/glass and (b) TiO_2/RR4-CS/glass systems.

3.5. Catalyst recyclability

Very few studies actually reported the reusability of dye-modified TiO_2 photocatalyst systems. Even so, the degradation of the target pollutants tends to slow down after several applications due to the leaching or photobleaching of the dye that retards the overall photocatalytic reaction. For example, Zyoud et al. [10] reported that the photocatalytic degradation of methyl orange by activated carbon/TiO_2/anthocyanin system decreases by 15% upon recovery, while Yang and Chan [34] found that the removal efficiencies of Cr(VI) by nanoscale ZnO sensitized by Alizarin Red S dye reduces from 75 to 50%.

In order to demonstrate that the immobilized TiO_2/RR4-CS layer-by-layer system is sustainable and stable, a study on the reusability of the immobilized photocatalyst systems was performed. This is important in order to assess the sustainability, reusability, and cost-effectiveness of the system. The reusability of the TiO_2/glass, TiO_2/CS/glass, and TiO_2/RR4-CS/glass systems throughout from the first to fifth cycles of applications is shown in Fig. 9.

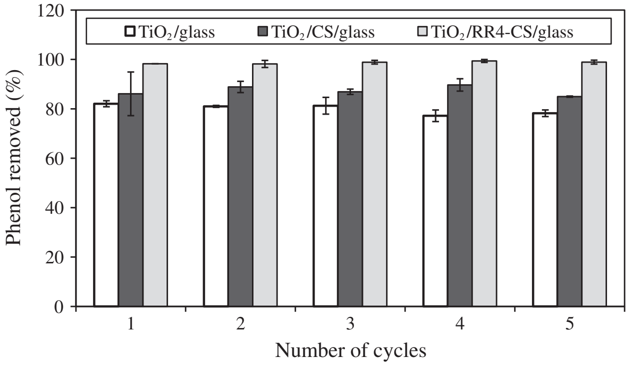

Fig. 9. The reusability of the immobilized photocatalyst systems on the percentage of phenol removed at ambient pH (6.6) with TiO_2 loading of 0.98 mg cm^{-2} and initial phenol concentration of 10 mg L^{-1}.

The result shows that the percentage of phenol removed by the TiO_2 single layer and TiO_2/CS layer-by-layer systems remained almost constant from the first to the fifth cycle with an average percentage of phenol removed of 80.0 ± 2.1% and 87.3 ± 2.0%, respectively. The best condition of phenol degradation was achieved by the TiO_2/RR4-CS layer-by-layer system. Under the operation of this photocatalyst system, the removal of phenol was maintained at almost 100% for up to five cycles of usage with a sustainable degradation rate of 0.033 ± 0.002 min^{-1} from the first cycle up to the fifth cycle.

The degradation efficiency of the TiO_2/RR4-CS layer-by-layer system was due to the existence of two processes occurring at the same time (photocatalysis and charge transfer) [17]. Besides that, the TiO_2/RR4-CS/glass system was also highly reusable and stable under the studied conditions. There was also no occurrence of any desorption or leaching of the adsorbed dye within the CS sub-layer into the treated aqueous solution. On the other hand, the degradation of phenol by the TiO_2/CS layer-by-layer system only improved slightly as compared to the TiO_2 single layer system. In this case, CS only acts as the immobilization substrate for the dye and was not involved in the electron transfer process as CS did not undergo photooxidation.

3.6. Photocatalytic efficiency for the removal of phenol intermediates

The degradation of phenol took place in multiple steps and resulted in several byproducts before it could be completely mineralized to CO_2 and H_2O. The main intermediates produced during the photocatalytic degradation of phenol (PhOH) by the TiO_2 single layer, TiO_2/CS, and TiO_2/RR4-CS layer-by-layer systems were identified as hydroquinone (HQ), catechol (CAT), and maleic (MAL) acid. The same intermediates were also observed by Jawad and Nawi [14].

Fig. 10(a)–(c) shows the time course of PhOH and the main intermediates detected from the HPLC (HQ, CAT, MAL acid) during the photocatalytic degradation of PhOH by the TiO_2/glass, TiO_2/CS/glass, and TiO_2/RR4-CS/glass systems, respectively. As can be seen, the intermediates appeared as soon as PhOH started to degrade. However, TiO_2 single layer and TiO_2/CS layer-by-layer systems demonstrated the poorest photocatalytic efficiency towards the removal of PhOH and its intermediates. For example, after 120 min of irradiation, PhOH and its intermediates still appeared in considerable quantities. This is unfavorable since HQ and CAT are considered toxic and an inhibitory intermediate, respectively [35].

On the other hand, the TiO_2/RR4-CS layer-by-layer system exhibited better photocatalytic efficiency in terms of PhOH removal and its intermediates whereby complete removal of PhOH and most of its intermediates was achieved within 120 min of irradiation time. Only MAL acid was still detectable by the end of the reaction time. This is also supported by the fact that the pH of the solution decreases from 6.8 to 3.8 at the end of the reaction time, caused by the formation of organic acids [36]. This observation indicates that aromatic intermediates were more degradable than carboxylic acids, which appears to be more resistant to oxidation under these operating conditions. MAL acid is an inert and non-biodegradable carboxylic acid, but

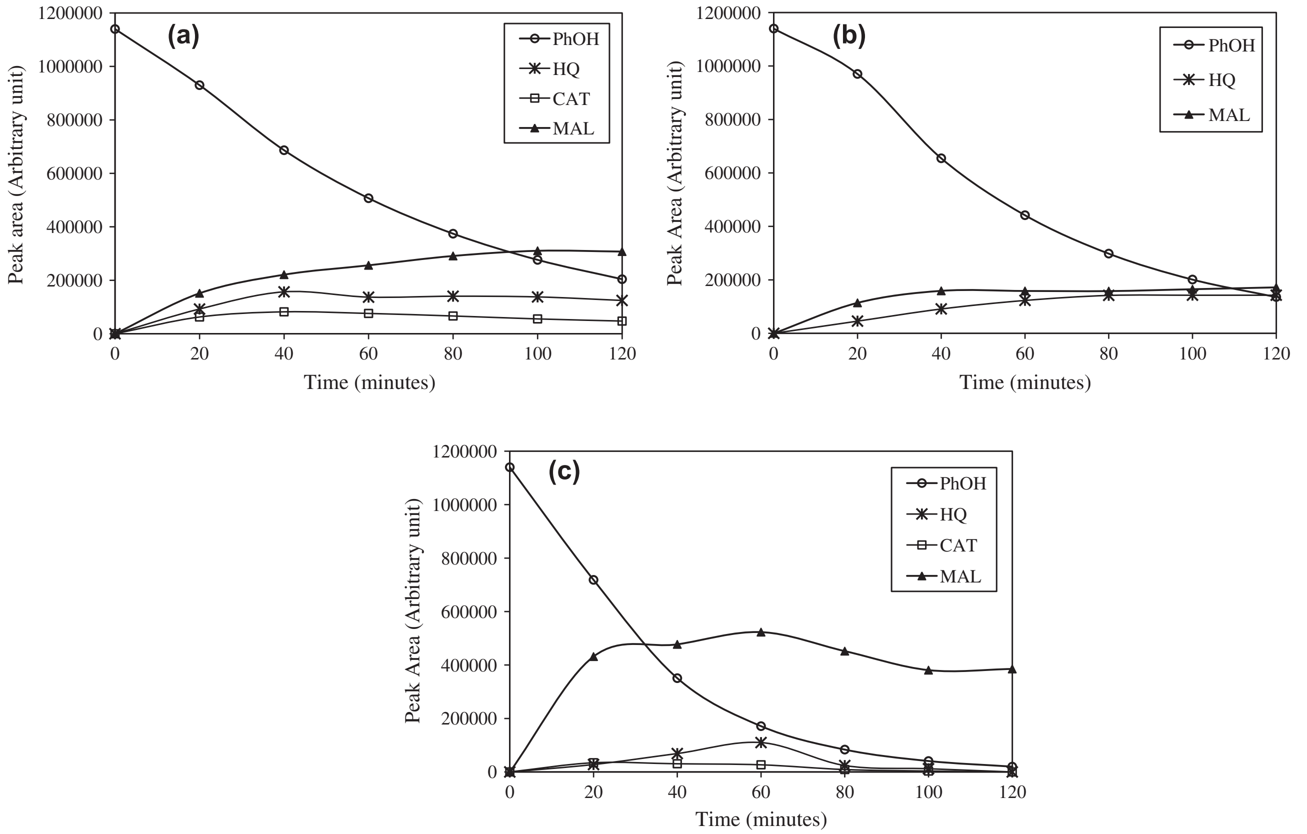

Fig. 10. The time course of PhOH and its main intermediates detected from HPLC by the (a) TiO_2/glass, (b) TiO_2/CS/glass, and (c) TiO_2/RR4-CS/glass systems, respectively, during the photocatalytic degradation of PhOH.

it is not toxic [35]. It could slowly be degraded to oxalic, acetic, and formic acids by extending the reaction time, which would eventually lead to complete mineralization to CO_2 and H_2O [37–40].

4. Conclusions

In this study, an immobilized TiO_2/CS loaded with RR4 dye has been successfully fabricated via a layer-by-layer assemblage system. The optimum loading of TiO_2 obtained was 0.98 mg cm^{-2} (equivalent to 14.5 ± 0.4 μm of thickness). Catalyst loading or thickness higher than the optimum value was found to be detrimental on the photocatalytic degradation of phenol. Photo-etching of the photocatalyst systems for 10 h enhanced the photocatalytic degradation of phenol by fourfold due to the formation of the macropores within the surface of TiO_2. Application of the TiO_2/RR4-CS layer-by-layer system for the photocatalytic degradation of phenol and its intermediates showed better photocatalytic performance than the TiO_2 single layer and TiO_2/CS layer-by-layer systems. In this case, complete removal of phenol could be achieved by the TiO_2/RR4-CS layer-by-layer system within 2 h of reaction time. The improved photocatalytic activity of the immobilized TiO_2/RR4-CS layer-by-layer system was due to photocatalytic and charge transfer processes occurring simultaneously. The charge transfer process provides better charge separation and lower electron–hole pair recombination of the TiO_2/RR4-CS layer-by-layer system. Besides having good photocatalytic performance, the leaching as well as direct oxidation of the chemisorbed dye were prevented by the layer-by-layer assemblage system. Furthermore, the immobilized TiO_2/RR4-CS layer-by-layer system was also readily recovered from the reaction mixture and reusable for at least five cycles of extended use without losing its efficiency.

Acknowledgments

The authors are grateful to the Ministry of Science, Technology and Innovation (MOSTI) Malaysia and Ministry of Higher Education (MOHE) Malaysia, for supporting this project under Science Fund Grant (305/PKIMIA/613402) and FRGS grant (203/PKIMIA/671027), respectively. We would also like to acknowledge Universiti Sains Malaysia (USM) for the USM Fellowship and Research University Postgraduate Research Grant Scheme (USM-RU-PGRS, 1001/PKIMIA/842070) granted to S. Sabar.

References

[1] R. Janisch, P. Gopal, N.A. Spaldin, Transition metal-doped TiO_2 and ZnO—Present status of the field, J. Phys. Condens. Matter 17 (2005) R657–R689.

[2] C.M. Teh, A.R. Mohamed, Roles of titanium dioxide and ion-doped titanium dioxide on photocatalytic degradation of organic pollutants (phenolic compounds and dyes) in aqueous solutions: A review, J. Alloys Compd. 509 (2011) 1648–1660.

[3] M.S. Kim, G. Liu, W.K. Nam, B.W. Kim, Preparation of porous carbon-doped TiO_2 film by sol–gel method and its application for the removal of gaseous toluene in the optical fiber reactor, J. Ind. Eng. Chem. 17 (2011) 223–228.

[4] P.A. Mangrulkar, S.P. Kamble, M.M. Joshi, J.S. Meshram, N.K. Labhsetwar, S.S. Rayalu, Photocatalytic degradation of phenolics by N-doped mesoporous titania under solar radiation, Int. J. Photoenergy 2012 (2012) p. 10.

[5] W.S. Kuo, Y.H. Chiang, L.S. Lai, Solar photocatalysis of carbaryl rinsate promoted by dye photosensitization, Dyes Pigm. 76 (2008) 82–87.

[6] R. Vinu, S. Polisetti, G. Madras, Dye sensitized visible light degradation of phenolic compounds, Chem. Eng. J. 165 (2010) 784–797.

[7] S. Kaur, V. Singh, Visible light induced sonophotocatalytic degradation of Reactive Red dye 198 using dye sensitized TiO_2, Ultrason. Sonochem. 14 (2007) 531–537.

[8] G. Qin, Z. Sun, Q. Wu, L. Lin, M. Liang, S. Xue, Dye-sensitized TiO_2 film with bifunctionalized zones for photocatalytic degradation of 4-chlorophenol, J. Hazard. Mater. 192 (2011) 599–604.

[9] H.S. Hilal, L.Z. Majjad, N. Zaatar, A. El-Hamouz, Dye-effect in TiO_2 catalyzed contaminant photo-degradation: Sensitization vs. charge-transfer formalism, Solid State Sci. 9 (2007) 9–15.

[10] A. Zyoud, N. Zaatar, I. Saadeddin, M.H. Helal, G. Campet, M. Hakim, D. Park, H.S. Hilal, Alternative natural dyes in water purification: Anthocyanin as TiO_2-sensitizer in methyl orange photo-degradation, Solid State Sci. 13 (2011) 1268–1275.

[11] M.Y. Chang, R.S. Juang, Equilibrium and kinetic studies on the adsorption of surfactant, organic acids and dyes from water onto natural biopolymers, Colloids Surf. A 269 (2005) 35–46.

[12] M.A. Nawi, S. Sabar, A.H. Jawad, Sheilatina, W.S.W. Ngah, Adsorption of Reactive Red 4 by immobilized chitosan on glass plates: Towards the design of immobilized TiO_2–chitosan synergistic photocatalyst-adsorption bilayer system, Biochem. Eng. J. 49 (2010) 317–325.

[13] R. Bonnett, M.A. Krysteva, I.G. Lalov, S.V. Artarsky, Water disinfection using photosensitizers immobilized on chitosan, Water Res. 40 (2006) 1269–1275.

[14] A.H. Jawad, M.A. Nawi, Fabrication, optimization and application of an immobilized layer-by-layer TiO_2/chitosan system for the removal of phenol and its intermediates under 45-W fluorescent lamp, React. Kinet. Mech. Catal. 106 (2011) 1–17.

[15] Z. Zainal, L.K. Hui, M.Z. Hussein, A.H. Abdullah, I.R. Hamadneh, Characterization of TiO_2–chitosan/glass photocatalyst for the removal of a monoazo dye via photodegradation–adsorption process, J. Hazard. Mater. 164 (2009) 138–145.

[16] Y. Chen, D.D. Dionysiou, Correlation of structural properties and film thickness to photocatalytic activity of thick TiO_2 films coated on stainless steel, Appl. Catal. B 69 (2006) 24–33.
[17] M.A. Nawi, S. Sabar, Sheilatina, Photocatalytic decolourisation of Reactive Red 4 dye by an immobilised TiO_2/chitosan layer by layer system, J. Colloid Interface Sci. 372 (2012) 80–87.
[18] A. Mills, S.K. Lee, A. Lepre, I.P. Parkin, S.A. O'Neill, Spectral and photocatalytic characteristics of TiO_2 CVD films on quartz, Photochem. Photobiol. Sci. 1 (2002) 865–868.
[19] J. Shang, W. Yao, Y. Zhu, N. Wu, Structure and photocatalytic performances of glass/SnO_2/TiO_2 interface composite film, Appl. Catal. A 257 (2004) 25–32.
[20] L. Caballero, K.A. Whitehead, N.S. Allen, J. Verran, Inactivation of *Escherichia coli* on immobilized TiO_2 using fluorescent light, J. Photochem. Photobiol. 202 (2009) 92–98.
[21] M.A. Nawi, A.H. Jawad, S. Sabar, W.S.W. Ngah, Photocatalytic-oxidation of solid state chitosan by immobilized bilayer assembly of TiO_2-chitosan under a compact household fluorescent lamp irradiation, Carbohydr. Polym. 83 (2011) 1146–1152.
[22] C.H. Chiou, C.Y. Wu, R.S. Juang, Influence of operating parameters on photocatalytic degradation of phenol in UV/TiO_2 process, Chem. Eng. J. 139 (2008) 322–329.
[23] A.H. Jawad, M.A. Nawi, Oxidation of crosslinked chitosan-epichlorohydrine film and its application with TiO_2 for phenol removal, Carbohydr. Polym. 90 (2012) 87–94.
[24] A.H. Jawad, M.A. Nawi, Characterizations of the photocatalytically-oxidized cross-Linked chitosan-glutaraldehyde and its application as a sub-layer in the TiO_2/CS-GLA bilayer photocatalyst system, J. Polym. Environ. 20 (2012) 817–829.
[25] I. Zainol, H.M. Akil, A. Mastor, Effect of γ-irradiation on the physical and mechanical properties of chitosan powder, Mater. Sci. Eng. C 29 (2009) 292–297.
[26] M.A. Nawi, Y.S. Ngoh, S.M. Zain, Photoetching of immobilized TiO_2–ENR_{50}–PVC composite for improved photocatalytic activity, Int. J. Photoenergy 2012 (2012) p. 12.
[27] M.A. Nawi, S.M. Zain, Enhancing the surface properties of the immobilized Degussa P-25 TiO_2 for the efficient photocatalytic removal of methylene blue from aqueous solution, Appl. Surf. Sci. 258 (2012) 6148–6157.
[28] M.A. Nawi, A.H. Jawad, S. Sabar, W.S.W. Ngah, Immobilized bilayer TiO_2/chitosan system for the removal of phenol under irradiation by a 45 watt compact fluorescent lamp, Desalination 280 (2011) 288–296.
[29] L. Huang, M. Zhai, J. Peng, J. Li, G. Wei, Radiation-induced degradation of carboxymethylated chitosan in aqueous solution, Carbohydr. Polym. 67 (2007) 305–312.
[30] W. Yue, R. He, P. Yao, Y. Wei, Ultraviolet radiation-induced accelerated degradation of chitosan by ozone treatment, Carbohydr. Polym. 77 (2009) 639–642.
[31] N.N. Duy, D.V. Phu, N.T. Anh, N.Q. Hien, Synergistic degradation to prepare oligochitosan by γ-irradiation of chitosan solution in the presence of hydrogen peroxide, Radiat. Phys. Chem. 80 (2011) 848–853.
[32] N.Q. Hien, D.V. Phu, N.N. Duy, N.T.K. Lan, Degradation of chitosan in solution by gamma irradiation in the presence of hydrogen peroxide, Carbohydr. Polym. 87 (2012) 935–938.
[33] G. Mascolo, R. Comparelli, M.L. Curri, G. Lovecchio, A. Lopez, A. Agostiano, Photocatalytic degradation of methyl red by TiO_2: Comparison of the efficiency of immobilized nanoparticles versus conventional suspended catalyst, J. Hazard. Mater. 142 (2007) 130–137.
[34] G.C.C. Yang, S.W. Chan, Photocatalytic reduction of chromium(VI) in aqueous solution using dye-sensitized nanoscale ZnO under visible light irradiation, J. Nanopart. Res. 11 (2009) 221–230.
[35] M.E. Suarez-Ojeda, A. Guisasola, J.A. Baeza, A. Fabregat, F. Stüber, A. Fortuny, J. Font, J. Carrera, Integrated catalytic wet air oxidation and aerobic biological treatment in a municipal WWTP of a high-strength *o*-cresol wastewater, Chemosphere 66 (2007) 2096–2105.
[36] R. Alnaizy, A. Akgerman, Advanced oxidation of phenolic compounds, Adv. Environ. Res. 4 (2000) 233–244.
[37] E. Grabowska, J. Reszczyńska, A. Zaleska, Mechanism of phenol photodegradation in the presence of pure and modified-TiO_2: A review, Water Res. 46 (2012) 5453–5471.
[38] A. Rey, J. Carbajo, C. Adán, M. Faraldos, A. Bahamonde, J.A. Casas, J.J. Rodriguez, Improved mineralization by combined advanced oxidation processes, Chem. Eng. J. 174 (2011) 134–142.
[39] A. Rey, J. Carbajo, C. Adán, M. Faraldos, A. Bahamonde, J.A. Casas, J.J. Rodriguez, Improved mineralization by combined advanced oxidation processes, Chem. Eng. J. 174 (2011) 134–142.
[40] M. Pimentel, N. Oturan, M. Dezotti, M.A. Oturan, Phenol degradation by advanced electrochemical oxidation process electro-Fenton using a carbon felt cathode, Appl. Catal. B 83 (2008) 140–149.